Optimum Performance of Nonlinear OFDM Schemes

João Guerreiro, Rui Dinis, *Senior Member, IEEE*, and Paulo Montezuma

***Abstract*—It is widely recognized that OFDM (Orthogonal Frequency Division Multiplexing) signals are very prone to nonlinear distortion effects, which can lead to significant performance degradation. However, recent results have showed that nonlinear distortion effects do not necessarily mean performance degradation and can actually lead to performance improvements relatively to conventional, linear OFDM schemes. In this paper we consider the effects of bandpass memoryless nonlinear devices on OFDM signals and study the optimum asymptotic performance for both non-dispersive channels and severely time-dispersive channels. We present analytical methods for obtaining the Euclidean distance between two OFDM signals that are subjected to different nonlinear characteristics. These results are then employed for obtaining the average asymptotic gain relatively to conventional, linear OFDM schemes in non-dispersive channels and the gain distribution for severely time-dispersive channels with Rayleigh-distributed fading on the different multipath components. Our analytical results, which are shown to be very accurate, indicate that the optimum detection of OFDM schemes with strong nonlinear distortion effects allows significant gains when compared with conventional, linear OFDM schemes.** [1]

***Index Terms*—Optimum detection, OFDM signals, nonlinear distortion, performance evaluation.**

I. Introduction

OFDM modulations [1] have become very popular for current wireless communications systems. They are employed in many wireless communications standards such as DVB (Digital Video Broadcasting) [2], LTE (Long Term Evolution) [3] and WiMAX (Worldwide Interoperability for Microwave Access) [4]. This choice is based on two key advantages of OFDM schemes: (i) their high spectral efficiency and, (ii) their facility to deal with frequency-selective channels without the need for complex receivers.

However, OFDM signals have large envelope fluctuations and, consequently, a high PAPR (Peak-to-Average Power Ratio). This leads to the saturation of the power amplifier, and, consequently, nonlinear distortion effects at the transmitter output. To deal with the high power peaks of OFDM signals and avoid the saturation of the power amplifier, a high IBO (Input Back-Off) can be considered. However, high IBOs lead to lower amplification efficiencies since the power amplifier works far from its saturation point. For this reason, several techniques to mitigate the high PAPR of OFDM signals have been proposed in the literature (see [5] and the references within). Among the proposed techniques, the simplest and more flexible ones involve the use of a nonlinear operation in the time-domain, followed by a filtering operation to eliminate the out-of-band radiation and maintain the original signal bandwidth [6]. However, although the resultant signal has a lower PAPR and allows a more efficient power amplification, it is also impaired by nonlinear distortion.

For these reasons, the existence of nonlinear distortion effects in OFDM signals is almost unavoidable. The nonlinear devices present in the transmission chain are commonly modeled as bandpass memoryless nonlinearities and can either be unintentional, as when we employ nonlinear amplifiers [7], or intentional, such as the ones inherent to the use of PAPR-reducing clipping techniques [6],[8][9].

To study the impact of nonlinear distortion effects on OFDM signals, one can take advantage of their Gaussian nature specially when the number of subcarriers is high. Under the Gaussian approximation, the Bussgang theorem [10][11] states that a nonlinearly distorted signal can be decomposed in two uncorrelated terms: one that is proportional to the original signal and another that represents the nonlinear distortion and aggregates the content of all inter modulation products. There are basically three approaches to deal with the nonlinear distortion:

- Consider it as an additional noise component that leads to performance degradation. This degradation can be specially serious when we have strong nonlinear distortion effects and/or for larger constellations;
- Employ receivers that try to estimate and cancel this distortion sometimes denoted as "Bussgang Receivers" [12]-[15]. However, these receivers have limitations since the estimation of the distortion term is not easy, especially at low SNR (Signal-to-Noise Ratio);
- Take advantage of the useful information in the nonlinear distortion component, which can be employed to improve the performance of the nonlinear OFDM schemes. As far as we know, the first work that considered this approach is [16], but the authors only studied the gains that are inherent to the diversity introduced by the nonlinearity. In fact, the optimum performance of nonlinear OFDM schemes can be as good or even better than the performance of conventional linear OFDM schemes [17] even in AWGN (Additive White Gaussian Noise) channels, which reveals performance improvements beyond the diversity gains of [16]. Several sub-optimum receivers were proposed to approach this optimum performance [16]-[19].

Manuscript received January X, 2014; revised January X, 2014. This work was supported by Instituto de Telecomunicações and Fundação para a Ciência e Tecnologia (FCT) under the project ADIN (PTDC/EEI-TEL/2990/2012) and the grant SFRH/BD/90997/2012.

João Guerreiro is with Faculdade de Ciências e Tecnologia (FCT), Monte de Caparica, Portugal.

Rui Dinis is with Instituto de Telecomunicações, Lisboa, Portugal and Faculdade de Ciências e Tecnologia (FCT), Monte de Caparica, Portugal.

Paulo Montezuma is with UNINOVA, Monte de Caparica, Portugal and Faculdade de Ciências e Tecnologia (FCT), Monte de Caparica, Portugal.

[1]Part of this work was published at VTC'2013 (Spring).

In this paper we consider OFDM signals with strong nonlinear distortion effects and we extend the results of [17] to a wide range of bandpass memoryless nonlinearities. We study the average asymptotic gain associated to the optimum detection since it provides a good reference for the performance with an optimum detection, specially when the number of subcarriers is large. This study comprises both non-dispersive channels and severely time-dispersive channels and present analytical methods for obtaining the Euclidean distance between two OFDM signals that are subjected to different nonlinear characteristics. These results are then employed for obtaining the average asymptotic gain relatively to conventional, linear OFDM schemes in non-dispersive channels and the gain distribution for severely time-dispersive channels with Rayleigh-distributed fading on the different multipath components. The major contributions of this paper are the following:

- Analytical evaluation of the average asymptotic gain in an ideal non-dispersive channel when there are bandpass memoryless nonlinearities (both intentional and unintentional) in the transmission chain. This can be regarded as an extension of the results presented in [17], since the bandpass memoryless nonlinearities considered there (with only AM/AM (Amplitude Modulation/Amplitude Modulation) nonlinear distortion) can be regarded as a special kind of bandpass nonlinearities without AM/PM (Amplitude Modulation/Phase Modulation) distortion effects;
- Analytical distribution of the gains for time-dispersive Rayleigh fading channels;
- Analytical computation of the average Euclidean distances and gain distributions for data blocks differing in more than one bit, something critical when we consider channel coding.

The paper is organized as follows: The nonlinear OFDM chain and the characterization of the signals along its blocks is made in Sec. II. The optimum detection of nonlinearly distorted OFDM signals is considered in Sec. III and Sec. IV presents an analytical method for obtaining the average asymptotic gains in ideal, non-dispersive channels. Sec. V shows how we can use these results for obtaining the gain distributions in frequency-selective channels and, finally, Sec. VI concludes the paper.

Throughout the paper the following conventions are adopted: bold letters denote matrices or vectors. Italic letters denote scalars. Capital letters are associated to the frequency-domain and small letters are associated to the time-domain. $||\mathbf{X}||$ denotes the Euclidean norm of the vector $\mathbf{X}$ and $(\cdot)^T$ denotes the transpose operator. $X_{i,j}$ denotes the element on the i^{th} line and j^{th} column of matrix $\mathbf{X}$. The PDF (Probability Density Function) of the random variable x, $p_x(x)$, is simply denoted by $p(x)$ when there is no risk of ambiguity. $\mathbb{E}[\cdot]$ denotes the average value.

II. Nonlinear OFDM Transmission

In this section we characterize the signals along the transmission chain depicted in Fig. 1. The input data signal is represented by the vector $\mathbf{S} = [S_0\, S_1\, ...\, S_{NM-1}]^T \in \mathbb{C}^{NM}$, which is a frequency-domain vector composed by N data symbols, each one selected from a QPSK (Quadrature Phase Shift Keying) constellation, plus $(M-1)N$ idle subcarriers at the edge of useful band, where M represents the oversampling factor. A time-domain version of $\mathbf{S}$ is obtained by applying an IDFT (Inverse Discrete Fourier Transform) to $\mathbf{S}$, i.e., $\mathbf{s} = \mathbf{F}^{-1}\mathbf{S} = [s_0\ s_1\ ...\ s_{NM-1}]^T \in \mathbb{C}^{NM}$ with $\mathbf{F}$ denoting the NM-point DFT (Discrete Fourier Transform) matrix, whose the entry at the i^{th} line and j^{th} column is given by[2]

$$F_{i,j} = \frac{1}{\sqrt{NM}} \exp\left(-\frac{j2\pi ij}{NM}\right), \quad i,j = 0,1,...MN-1. \tag{1}$$

The time-domain samples $\mathbf{s} = [s_0\ s_1\ ...\ s_{NM-1}]^T \in \mathbb{C}^{NM}$ have a Gaussian nature and can be modeled by a complex normal random variable, i.e., $s \sim \mathcal{CN}(0, 2\sigma^2)$. The absolute values of the time-domain samples are represented by $\mathbf{R} = |\mathbf{s}| = [R_0\ R_1\ ...\ R_{NM-1}]^T \in \mathbb{R}^{NM}$ and can be modeled by R, which is a random variable with Rayleigh distribution, i.e., the corresponding PDF is

$$p(R) = \frac{R}{\sigma^2} \exp\left(-\frac{R^2}{2\sigma^2}\right) u(R), \tag{2}$$

with $u(R)$ denoting the unitary step function. The polar memoryless nonlinearities considered in this work are characterized by the AM/AM and the AM/PM conversion functions that are represented by $A(\cdot)$ and $\Theta(\cdot)$, respectively. These functions only depend on the absolute value of the time-domain signal at their input. In Fig. 2 is depicted the scheme of a general bandpass memoryless nonlinearity. The n^{th} output sample is

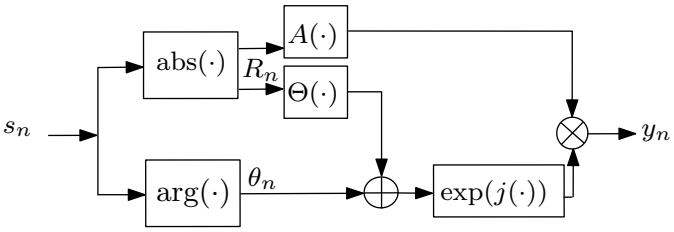

Fig. 2: General scheme of a polar memoryless nonlinearity.

given by

$$y_n = f(R_n)\exp(j\theta_n) = A(R_n)\exp(j(\Theta(R_n)+\theta_n)), \tag{3}$$

with $\theta_n = \arg(s_n)$ representing the original phase of the n^{th} time-domain sample. Throughout this work, we considered three bandpass memoryless nonlinearities: an ideal envelope clipping, a SSPA (Solid-State Power Amplifier) [20] and a TWTA (Traveling Wave Tube Amplifier) [7]. The SSPA is characterized by

$$A(R_n) = \frac{R_n}{\sqrt[2p]{\left(1+\left(\frac{R_n}{s_M}\right)^{2p}\right)}}, \tag{4}$$

and $\Theta(R_n) \approx 0$. The parameter p controls the smoothness between the linear region and the saturation, where the input and output envelope are both s_M. As we increase p we get

[2]It should be noted that the matrix indexes start in 0, instead of 1.

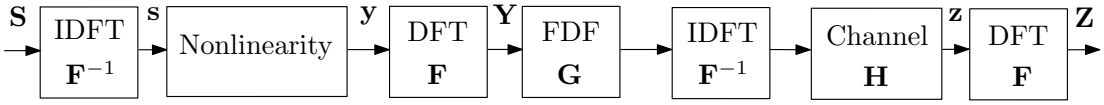

Fig. 1: Considered transmission scenario.

stronger nonlinear distortion effects and, in the limit, $p = +\infty$ and the SSPA turns into an ideal envelope clipping. The TWTA has the following AM/AM characteristic

$$A(R_n) = 2\frac{\frac{R_n}{s_M}}{1+\left(\frac{R_n}{s_M}\right)^2}, \tag{5}$$

and its AM/PM conversion function is

$$\Theta(R_n) = 2\frac{\theta_M\left(\frac{R_n}{s_M}\right)^2}{1+\left(\frac{R_n}{s_M}\right)^2}, \tag{6}$$

where s_M is the input and output amplitude at saturation and θ_M is the phase rotation added to the original input phase.

By taking advantage of the Gaussian nature of OFDM signals, the Bussgang theorem [10][11] can be used. In these conditions, the nonlinearly distorted signal at the nonlinearity output can be expressed as

$$\mathbf{y} = \alpha\mathbf{s} + \mathbf{d}, \tag{7}$$

where $\mathbf{d} = [d_0 \ d_1 \ ... \ d_{NM-1}]^T \in \mathbb{C}^{NM}$ represents the distortion introduced by the nonlinearity and α is an appropriate scale factor that relates the cross-correlation between the input and the output signals of the nonlinearity and the autocorrelation of the input signal,

$$\alpha = \frac{\mathbb{E}[s_n y_n^*]}{\mathbb{E}[|s_n|^2]}. \tag{8}$$

It is important to note that $\mathbb{E}[d_n] = 0$ and $\mathbb{E}[s_n d_n^*] = 0$, i.e., the distortion term has zero mean and is uncorrelated with the useful data. Making use of DFT definition in (1), the frequency-domain version of (7) is obtained through $\mathbf{Y} = \mathbf{F}\mathbf{y}$, that yields

$$\mathbf{Y} = \alpha\mathbf{S} + \mathbf{D}, \tag{9}$$

where $\mathbf{D} = [D_0 \ D_1 \ ... \ D_{NM-1}]^T \in \mathbb{C}^{NM}$ is the frequency-domain version of the distortion term that follows a normal distribution with zero mean as shown in [6][21][22]. In order to reduce the out-of-band radiation introduced by the nonlinearity, a FDF (Frequency Domain Filter) can be employed. In our signal processing scheme, this filtering operation is represented as a multiplication by the diagonal matrix $\mathbf{G}$, defined as

$$\mathbf{G} = \text{diag}\left(\left[\underbrace{0.....0}_{(M-1)N/2} \ \underbrace{1.....1}_{N} \ \underbrace{0.....0}_{(M-1)N/2}\right]^T\right). \tag{10}$$

When the filtering operation is not considered $\mathbf{G}$ is the identity matrix, i.e., $\mathbf{G} = \mathbf{I}$. Before the transmission, we attach an appropriate CP (Cyclic Prefix) to the time-domain block $\mathbf{F}^{-1}\mathbf{G}\mathbf{Y}$. The CP is assumed to be longer than the overall channel impulse response length, since for a shorter CP we have ISI and ICI effects [23][24]. At the reception side, the CP samples are discarded and we have $\mathbf{z} = [z_0 \ z_1 \ ... \ z_{NM-1}]^T \in \mathbb{C}^{NM}$, with the corresponding frequency-domain block $\mathbf{Z} = [Z_0 \ Z_1 \ ... \ Z_{NM-1}]^T \in \mathbb{C}^{NM}$ defined by

$$\mathbf{Z} = \alpha\mathbf{H}\mathbf{G}\mathbf{S} + \mathbf{H}\mathbf{G}\mathbf{D} + \mathbf{N}, \tag{11}$$

where $\mathbf{N} = [N_0 \ N_1 \ ... \ N_{NM-1}]^T \in \mathbb{C}^{NM}$ represents the noise components and $\mathbf{H} = \text{diag}\left([H_0 \ H_1 \ ... \ H_{NM-1}]^T\right)$ represents the channel frequency responses.

III. Optimum Detection

The nonlinear distortion component $\mathbf{d} = [d_0 \ d_1 \ ... \ d_{NM-1}]^T \in \mathbb{C}^{NM}$ (and the corresponding frequency-domain version $\mathbf{D} = [D_0 \ D_1 \ ... \ D_{NM-1}]^T \in \mathbb{C}^{NM}$) is usually regarded as an undesirable noise-like term that leads to performance degradation when conventional OFDM receivers (designed assuming linear OFDM transmissions) are employed. However, when we consider the optimum detection of nonlinearly distorted OFDM signals the situation is quite different [17]. In [17] is shown that the optimum receiver evaluates directly the Euclidean distance between the signals to choose the best estimate of the transmitted sequence and its performance is closely related to the minimum Euclidean distance between the transmitted signals. In this section we explain and show the potential gains inherent to an optimum detection of nonlinearly distorted OFDM signals. It is well known that obtaining analytically the optimum BER (Bit Error Rate) performance in this case is very difficult. Therefore, we need an accurate BER measure that can be obtained in a practical way. For this reason, we considered the asymptotic gain (or degradation) relatively to the linear case. Since the asymptotic gain can be associated to very rare events, we used its average value (i.e., we averaged it over different data sequences differing in a given number of bits), leading to what we called "average asymptotic gain". Since its variance is small, especially for large blocks (see Fig. 4 below), it provides an accurate insight of the optimum performance for low BER.

The main idea behind our approach is that when we have strong nonlinear distortion effects the ratio between the squared Euclidean distance and the average bit energy can be higher than in a scenario where the transmission is linear. Considering the existence of nonlinear distortion effects and the DFT definition in (1), we can define the average bit energy for QPSK constellations[3] in the frequency-domain as

$$E_b^{NL} = \frac{\sum_{k=0}^{NM-1}|Y_k|^2}{2N}. \tag{12}$$

[3]The generalization to other constellations is straightforward.

In the case of a linear transmission, the average bit energy is given by

$$E_b^L = \frac{\sum_{k=0}^{NM-1} |S_k|^2}{2N}. \quad (13)$$

To evaluate these potential gains, let us start by considering the data sequence $\mathbf{S}^{(2)} = [S_0^{(2)}\, S_1^{(2)}\, ...\, S_{NM-1}^{(2)}]^T \in \mathbb{C}^{NM}$ that differs from $\mathbf{S}^{(1)} = [S_0^{(1)}\, S_1^{(1)}\, ...\, S_{NM-1}^{(1)}]^T \in \mathbb{C}^{NM}$ in μ bits uncorrelated positioned on the subcarriers whose indexes define the set $\mathbf{\Phi} = [\Phi_0\, \Phi_1\, ...\, \Phi_{\mu-1}]$, with $\Phi_i \in \{0, N-1\}$. These two sequences are submitted to a bandpass memoryless nonlinearity to generate $\mathbf{Y}^{(2)}$ and $\mathbf{Y}^{(1)}$, respectively. Fig. 3 shows the absolute value of the difference between two nonlinearly distorted sequences that differ in one bit considering an ideal AWGN channel. From the figure, it

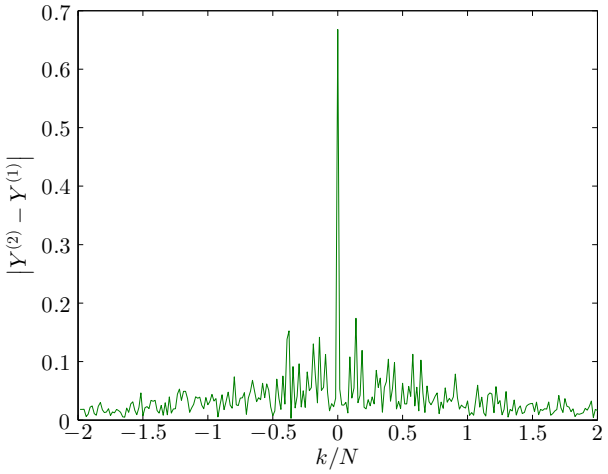

Fig. 3: Difference between two OFDM signals distorted by an ideal envelope clipping parametrized $s_M/\sigma = 0.5$.

can be noted that there exists power in all subcarriers and not only on the subcarrier where the bit was modified. This suggests the existence of a diversity gain as is pointed out in [16]. The potential energy gain that can be achieved without considering a FDF is related to the squared Euclidean distance with and without nonlinear distortion effects. When a linear transmission is considered, we have $\mathcal{D}_L^2 = 4E_b^L$. In the other hand, if there is a nonlinear transmission, the squared Euclidean distance is $\mathcal{D}_{NL}^2 = 4\mathcal{G}E_b^{NL}$, where $\mathcal{G}$ is the potential asymptotic gain associated with the optimum detection, given by

$$\mathcal{G} = \frac{\mathcal{D}_{NL}^2}{4E_b^{NL}} = \frac{\left|\left|\mathbf{Y}^{(2)} - \mathbf{Y}^{(1)}\right|\right|^2}{4E_b^{NL}} = \frac{\sum_{k=0}^{MN-1} \left|\alpha\left(S_k^{(2)} - S_k^{(1)}\right) + D_k^{(2)} - D_k^{(1)}\right|^2}{4E_b^{NL}}. \quad (14)$$

Fig. 4 shows the distribution of $\mathcal{G}$, $p(\mathcal{G})$, considering OFDM sequences that differ in μ bits and are nonlinearly distorted by an envelope clipping parameterized with $s_M/\sigma = 1.0$. From the figure, we note that $\mathcal{G}$ has fluctuations around its

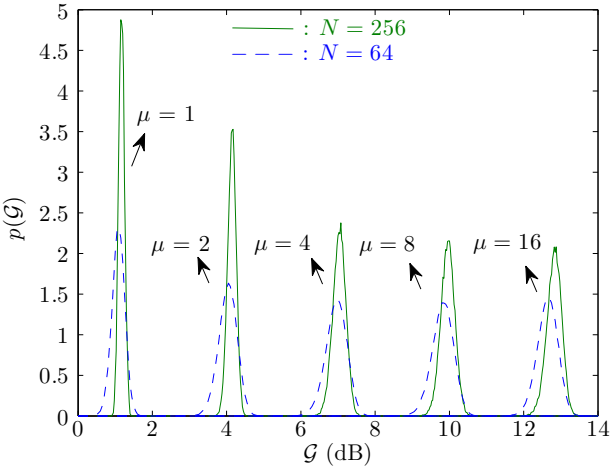

Fig. 4: PDF of $\mathcal{G}$ considering different values of μ and a variable number of in-band subcarriers N.

average value but they decrease as N increases. Moreover, the gain is almost always higher than 1 (the value for a linear transmission), i.e., $\mathbb{E}[\mathcal{G}]_{\mu=1} > 0$ dB. We also include the simulation of $p(\mathcal{G})$ for $\mu > 1$ since this is the typical situation of coded OFDM scenarios, where the minimum Euclidean distance is dominated by sequences that differ in $\mu > 1$ bits, with μ depending on the minimum Hamming distance of the code. It can be verified that even for $\mu > 1$ there are also potential performance improvements since $\mathbb{E}[\mathcal{G}]$ increases linearly with μ. Under the assumption that N is large, it is possible to approximate the Euclidean distance by the sum of two components: one associated to the useful part of the difference between the μ erroneous subcarriers, $\mathcal{D}_d^2$, and other associated to the distortion part of the difference between all subcarriers, $\mathcal{D}_c^2$,

$$\begin{aligned}\mathcal{D}_{NL}^2 &= \sum_{k=0}^{MN-1} \left|\alpha\left(S_k^{(2)} - S_k^{(1)}\right) + D_k^{(2)} - D_k^{(1)}\right|^2 \\ &\approx \sum_{k=0}^{MN-1} \left(\left|\alpha\left(S_k^{(2)} - S_k^{(1)}\right)\right|^2 + \mathbb{E}\left[\left|D_k^{(2)} - D_k^{(1)}\right|^2\right]\right) \\ &= \underbrace{\sum_{k\in\mathbf{\Phi}} \left|\alpha\left(S_k^{(2)} - S_k^{(1)}\right)\right|^2}_{\mathcal{D}_d^2} + \underbrace{\sum_{k=0}^{MN-1} \mathbb{E}\left[\left|D_k^{(2)} - D_k^{(1)}\right|^2\right]}_{\mathcal{D}_c^2}. \end{aligned} \quad (15)$$

For $D_k^{(i)}$ we have we $\sum_{k=0}^{MN-1} |D_k^{(i)}|^2 \approx \sum_{k=0}^{MN-1} \mathbb{E}[|D_k|^2]$ when $N \gg 1$ because different $D_k^{(i)}$ are almost uncorrelated, the expected values change slowly with k and we have a large number of terms in the second sum. Moreover the $D_k^{(i)}$ are uncorrelated with $S_k^{(i)}$ (Bussgang's theorem [10]). Finally, cross terms between $S_k^{(1)}$ and $D_k^{(2)}$ or $D_k^{(1)}$ and $S_k^{(2)}$ are also uncorrelated and with zero mean. With this approximation the asymptotic gain can be written as

$$\mathcal{G} \approx \underbrace{\frac{\mathcal{D}_d^2}{4E_b^{NL}}}_{\mathcal{G}_d} + \underbrace{\frac{\mathcal{D}_c^2}{4E_b^{NL}}}_{\mathcal{G}_c}, \quad (16)$$

i.e., we decompose the gain in two terms, one associated to the subcarriers where we have bit differences (where the nonlinear distortion term is much lower than the term associated to the "useful part"), and a second term associated to the subcarriers differing only in nonlinear distortion terms[4].

IV. Theoretical Optimum Asymptotic Performance

This section aims to present a theoretical characterization of the average potential gains presented in the previous section. In order to do this, let us start by introduce the error $\mathbf{E} = [E_0\, E_1\, ...\, E_{NM-1}]^T \in \mathbb{C}^{NM}$ between two modulated data sequences $\mathbf{S}^{(1)}$ and $\mathbf{S}^{(2)}$ by writing

$$\mathbf{S}^{(2)} = \mathbf{S}^{(1)} + \mathbf{E}. \tag{17}$$

The k^{th} element of $\mathbf{E}$ is given by

$$E_k = \begin{cases} d_{adj}\exp(j\nu), & k \in \mathbf{\Phi} \\ 0, & \text{otherwise}, \end{cases} \tag{18}$$

where d_{adj} is the minimum distance between two symbols of a given constellation C (in the concrete case of QPSK constellations we have $S_k = \pm 1 \pm j$, $d_{adj} = 2$ and $\nu \in \{0, \pi, \pm\pi/2\}$. Regarding the time-domain, the error term is represented by $\boldsymbol{\varepsilon} = \mathbf{F}^{-1}\mathbf{E} = [\varepsilon_0\, \varepsilon_1 \ldots \varepsilon_{NM-1}]^T \in \mathbb{C}^{NM}$, with the n^{th} element defined by

$$\begin{aligned} \varepsilon_n &= \sum_{k=0}^{MN-1} F_{n,k}^{-1} E_k = \sum_{k\in\mathbf{\Phi}} F_{n,k}^{-1} E_k \\ &= \sum_{k\in\mathbf{\Phi}} \frac{d_{adj}}{\sqrt{MN}} \exp\left(\frac{j2\pi nk}{MN} + j\nu\right) = \Delta_n \exp(j\phi_n). \end{aligned} \tag{19}$$

Let us model the absolutes value of the time-domain samples of the error term, $|\varepsilon_n| = \Delta_n$, with the random variable Δ, and their phases, $\arg(\varepsilon_n) = \phi_n$, with ϕ. It is important to note that although we do not have the distribution of Δ, $p(\Delta)$, it can be easily demonstrated that

$$\mathbb{E}[\Delta^2] = \frac{\mu}{NM} d_{adj}^2. \tag{20}$$

The random variable ϕ has uniform distribution in $[0 : 2\pi[$ and, consequently, its PDF is given by

$$p(\phi) = \frac{1}{2\pi}, \quad \phi \in [0 : 2\pi[, \tag{21}$$

and 0 otherwise. In order to derive the average asymptotic gain associated to the optimum detection, we present a theoretical expression for the average squared Euclidean distance between two nonlinearly distorted signals $\mathbf{Y}^{(1)}$ and $\mathbf{Y}^{(2)}$ associated to the submission of $\mathbf{S}^{(1)}$ and $\mathbf{S}^{(2)}$ to the memoryless nonlinearities presented in the Sec. II. Let us consider a time-domain sample of an OFDM signal in its polar form[5],

$$s = R\exp(j\theta), \tag{22}$$

and rewrite (19) as

$$\varepsilon = \Delta\exp(j\phi). \tag{23}$$

Applying an IDFT to (17), we have

$$R^{(2)}\exp\left(j\theta^{(2)}\right) = R^{(1)}\exp\left(j\theta^{(1)}\right) + \Delta\exp\left(j\phi\right). \tag{24}$$

Due to the circular nature of $s^{(1)}$ and ε we can assume without loss of generality that $\theta = 0$, leading to

$$\begin{aligned} R^{(2)}\exp\left(j\theta^{(2)}\right) &= R^{(1)} + \Delta\exp(j\phi) \\ &= \left(R^{(1)} + \Delta\cos(\phi)\right) + j\Delta\sin(\phi), \end{aligned}$$

as we can observe in Fig. 5. Defining $\Psi = \theta^{(2)} - \theta^{(1)}$, we

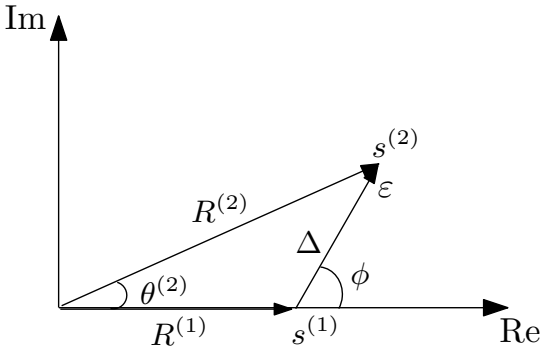

Fig. 5: Vectorial representation of $s^{(1)}$ and $s^{(2)}$ when $\theta^{(1)} = 0$.

have

$$\begin{aligned} \Psi &= \arg\left(R^{(1)} + \Delta\exp(j\phi)\right) = \arctan\left(\frac{\Delta\sin(\phi)}{R^{(1)} + \Delta\cos(\phi)}\right) \\ &\overset{(a)}{\approx} \frac{\Delta\sin(\phi)}{R^{(1)}}, \end{aligned} \tag{25}$$

where the approximation (a) is valid if $R^{(1)} \gg \Delta$. Similarly, $R^{(2)}$ can be approximated by

$$\begin{aligned} R^{(2)} &= \left|R^{(1)} + \Delta\exp(j\phi)\right| \\ &= \sqrt{(R^{(1)} + \Delta\cos(\phi))^2 + \Delta^2\sin^2(\phi)} \approx R^{(1)} + \Delta\cos(\phi). \end{aligned} \tag{26}$$

Regarding $s^{(1)}$, the nonlinearity output is hence

$$y^{(1)} = A\left(R^{(1)}\right)\exp\left(j\left(\theta^{(1)} + \Theta\left(R^{(1)}\right)\right)\right). \tag{27}$$

For $s^{(2)}$, assuming $\theta^{(2)} = 0$, we can write[6]

$$\begin{aligned} y^{(2)} &\approx A\left(R^{(2)}\right)\exp\left(j\left(\theta^{(2)} + \Theta(R^{(2)})\right)\right) \\ &= A\left(R + \Delta\cos(\phi)\right)\exp(j\Psi)\exp\left(j(\Theta(R + \Delta\cos(\phi))\right). \end{aligned} \tag{28}$$

Let us now express the nonlinearity in the Cartesian form as

$$\begin{aligned} f(R) &= A(R)\cos(\Theta(R)) + jA(R)\sin(\Theta(R)) \\ &= f_I(R) + jf_Q(R). \end{aligned} \tag{29}$$

[4]Due to distortion term in the μ subcarriers, this decomposition has an error of order μ/N that becomes negligible when $N \gg \mu$.

[5]Although we are working with time-domain samples, we omit the subscript n in the following equations for the sake of notation simplicity.

[6]Assuming $R^{(1)} = R$ for the sake of notation simplicity.

Using a Taylor approximation, we can expand $f_I(R + \Delta\cos(\phi))$ and $f_Q(R + \Delta\cos(\phi))$ around R, resulting,

$$f_I(R + \Delta\cos(\phi)) = f_I(R) + f_I'(R)\Delta\cos(\phi), \tag{30}$$

and,

$$f_Q(R + \Delta\cos(\phi)) = f_Q(R) + f_Q'(R)\Delta\cos(\phi). \tag{31}$$

With this approximation, the nonlinearity output for $s^{(2)}$ is $y^{(2)} \approx$

$$\Big(f_I(R) + f_I'(R)\Delta\cos(\phi) + j\big(f_Q(R) + f_Q'(R)\Delta\cos(\phi)\big)\Big) \times \exp(j\Psi). \tag{32}$$

For $s^{(1)}$, we can write

$$y^{(1)} = f_I(R) + jf_Q(R). \tag{33}$$

To obtain the Euclidean distance between these two signals, we will start by evaluating the difference between them, $y^{(2)} - y^{(1)} \approx$

$$\begin{aligned}
&\Big(f_I(R) + jf_Q(R) + \Delta\cos(\phi)\big(f_I'(R) + jf_Q'(R)\big)\Big)\exp(j\Psi) \\
&- \Big(f_I(R) + jf_Q(R)\Big) \\
&= \Big(f_I(R) + jf_Q(R)\Big)\Big(1 - \exp(-j\Psi)\Big) \\
&+ \Big(\Delta\cos(\phi)(f_I'(R) + jf_Q'(R))\Big) \\
&= A(R)\exp(j\Theta(R))\Big(1 - \exp(-j\Psi)\Big) \\
&+ \Big(\Delta\cos(\phi)(f_I'(R) + jf_Q'(R))\Big).
\end{aligned} \tag{34}$$

Recalling that $\sin(\Psi) \approx \Psi$ and $\cos(\Psi) \approx 1$ for low values of Ψ (say $\Psi \ll 1$) and using (25), we have $\exp(-j\Psi) \approx 1 - j\Psi \approx 1 - j\frac{\Delta\sin(\phi)}{R}$, which allows us to rewrite (34) as

$$\begin{aligned}
y^{(2)} - y^{(1)} \approx A(R)\exp\big(j\Theta(R)\big)j\left(\frac{\Delta\sin(\phi)}{R}\right) \\
+ \Delta\cos(\phi)\big(f_I'(R) + jf_Q'(R)\big).
\end{aligned} \tag{35}$$

Since

$$f_Q'(R) = A'(R)\sin(\Theta(R)) + A(R)\cos(\Theta(R))\Theta'(R), \tag{36}$$

and $f_I'(R) = f_Q'(R + \frac{\pi}{2})$, we can write $f_I'(R) + jf_Q'(R)$

$$\begin{aligned}
&= A'(R)\exp\big(j\Theta(R)\big) + A(R)\Theta'(R)\exp\left(j\left(\Theta(R) + \frac{\pi}{2}\right)\right) \\
&= \exp\big(j\Theta(R)\big)\big(A'(R) + jA(R)\Theta'(R)\big).
\end{aligned} \tag{37}$$

Using this result, (35) turns to

$$\begin{aligned}
y^{(2)} - y^{(1)} &\approx \Delta\exp\big(j\Theta(R)\big) \\
&\times \Big(j\frac{A(R)\sin(\phi)}{R} + \cos(\phi)\big(A'(R) + jA(R)\Theta'(R)\big)\Big).
\end{aligned} \tag{38}$$

The squared absolute value of (38) is

$$\begin{aligned}
\left|y^{(2)} - y^{(1)}\right|^2 &\approx \Delta^2\left(\big(A'(R)\cos(\phi)\big)^2\right) \\
&+ \Delta^2\left(\frac{A(R)\sin(\phi)}{R} + \big(\Theta'(R)A(R)\cos(\phi)\big)^2\right).
\end{aligned} \tag{39}$$

Considering Δ, ϕ and R to be independent, we can approximate the average value of the squared Euclidean distance between $\mathbf{y}^{(2)}$ and $\mathbf{y}^{(1)}$ as represented in (40) (on the top of the next page), given that $\mathbb{E}_\phi[\cos^2(\phi)] = \mathbb{E}_\phi[\sin^2(\phi)] = \mathbb{E}_\phi[\sin(2\phi)] = 1$. As R is Rayleigh distributed, the average bit energy is theoretically given by

$$E_b^{NL} = \frac{1}{2}\mathbb{E}[f^2(R)] = \frac{1}{2}\int_0^{+\infty} f^2(R)p(R)\mathrm{d}R. \tag{41}$$

Using (40) and (41), the average value of (14) can be theoretically obtained by

$$\begin{aligned}
\mathbb{E}[\mathcal{G}] &= \frac{\mathbb{E}[\mathcal{D}_{NL}^2]}{4E_b^{NL}} \\
&= \frac{\mu d_{adj}^2\displaystyle\int_0^{+\infty}\left(A'^2(R) + \frac{A^2(R)}{R^2} + \Theta'^2(R)A^2(R)\right)p(R)\mathrm{d}R}{2\displaystyle\int_0^{+\infty} f^2(R)p(R)\mathrm{d}R}.
\end{aligned} \tag{42}$$

It should be noted that when we do not have AM/PM distortion we have $\Theta(R) = 0$ and (42) reduces to the expression derived in [17]. Fig. 6 shows the average asymptotic gain of the optimum receiver considering a SSPA with $p = 1$ and a TWTA with $\theta_M = \pi/3$ as a function of s_M/σ. The OFDM signals have a variable number of N in-band subcarriers and $M = 4$. From this figure we note that the theoretical expression is very accurate for both nonlinearities. When N is large the error becomes lower than 0.2 dB since the Taylor approximations are more accurate. The bigger potential gains of the TWTA can be explained due to its stronger nonlinear distortion effects comparing to the SSPA with $p = 1$, which is a smooth nonlinearity. As we consider SSPA amplifiers with higher values of p, higher average asymptotic gains are expected. However, although the gain seems to increase when s_M/σ decreases, a very low value of s_M/σ can bring problems, especially when sub-optimal receivers are taken into account [17]. It also should be noted that when a TWTA is considered, $\mathbb{E}[\mathcal{G}]$ converges to 1 (0 dB) for large s_M/σ, although at a slower rate when compared to the SSPA case.

V. Performance of Optimum Receivers in Frequency-selective Channels

The work presented in the previous sections shows that there are gains associated with the optimum detection of nonlinearly distorted OFDM signals in ideal AWGN channels. However, OFDM schemes are commonly employed in dispersive channels rather than in non-dispersive channels. Thus, it is important to understand if the potential gains associated to the AWGN channels still exist in dispersive channels. In this section, we analyse the optimum performance of nonlinear OFDM schemes in severely time-dispersive channels by making use of their statistical behaviour. When dealing with frequency-selective channels the asymptotic gain associated to a nonlinear OFDM transmission (conditioned to a given channel realization $\mathbf{H}$) can be written as

$$\mathcal{G}_H = \frac{\mathcal{D}_{NL,H}^2}{4E_b^{NL}} \tag{43}$$

$$\mathbb{E}[\mathcal{D}_{NL}^2] \approx NM\mathbb{E}_{\Delta,R,\phi}\left[\Delta^2\left(\left(A'(R)\cos(\phi)\right)^2+\left(\frac{A(R)\sin(\phi)}{R}+\Theta'(R)A(R)\cos(\phi)\right)^2\right)\right]$$
$$= NM\left(\mathbb{E}_{\Delta}\left[\Delta^2\right]\mathbb{E}_R\left[A'^2(R)+\frac{A^2(R)}{R^2}+\Theta'^2(R)A^2(R)\right]\right)$$
$$= \mu d_{adj}^2\int_0^{+\infty}\left(A'^2(R)+\frac{A^2(R)}{R^2}+\Theta'^2(R)A^2(R)\right)p(R)\mathrm{d}R. \quad (40)$$

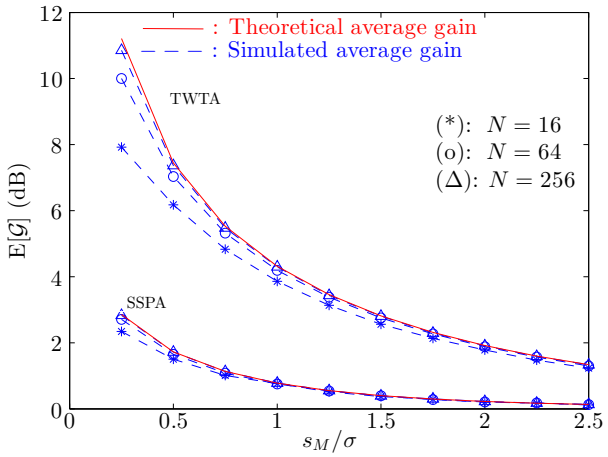

Fig. 6: Average asymptotic gain of a SSPA and a TWTA as a function of s_M/σ.

$$= \frac{\sum_{k=0}^{MN-1}|H_k|^2\left|\alpha\left(S_k^{(2)}-S_k^{(1)}\right)+D_k^{(2)}-D_k^{(1)}\right|^2}{4E_b^{NL}}$$
$$= \frac{\sum_{k=0}^{MN-1}|H_k|^2\mathcal{D}_{NL,k}^2}{4E_b^{NL}}.$$

It should be pointed out that the average bit energy is also conditioned to the channel realization but since we considered a normalized channel with $\mathbb{E}[|H_k|^2]=1$, E_b^{NL} is still given by (41).

To obtain (43) we first note that, as in (16), we can decompose it as $\mathcal{G}_H = \mathcal{G}_{H,d}+\mathcal{G}_{H,c}$, with the first term associated to the subcarriers where we have bit differences and the second term associated to the subcarriers where $\mathcal{D}_{NL,k}^2$ has only nonlinear distortion terms.

Clearly,

$$\mathcal{G}_{H,d} \approx \frac{\frac{\mathbb{E}[\mathcal{D}_d^2]}{\mu}\sum_{k\in\mathbf{\Phi}}|H_k|^2}{4E_b^{NL}} = \frac{\mathbb{E}[\mathcal{G}_d]\gamma_d}{\mu}, \quad (44)$$

where $\mathbb{E}[\mathcal{D}_d^2]$ is a function of the bit differences and

$$\gamma_d = \sum_{k\in\mathbf{\Phi}}|H_k|^2. \quad (45)$$

The computation of $\mathcal{G}_{H,d}$ is more difficult, since it has a term of the type $\sum_k|H_k|^2|D_k^{(1)}-D_k^{(2)}|^2 = \sum_k|H_k|^2\mathcal{D}_{d,k}^2$. To obtain it we should have in mind the following:

(a) $\mathcal{D}_{d,k}^2$ changes much faster than $|H_k|^2$ (see Fig. 7);
(b) $\mathcal{D}_{d,k}^2$ has a huge number of oscillations over the sum (see Fig. 7);
(c) The statistical properties $\mathcal{D}_{d,k}^2$ change very slowly over the sum, namely when compared with $|H_k|^2$;
(d) $|H_k|^2$ has a large number of oscillations;
(e) The sum of $|H_k|^2$ over a sliding window with length R, with $1 << R << N$ is almost constant and equal to $\frac{R}{N}\sum_k|H_k|^2$ [7].

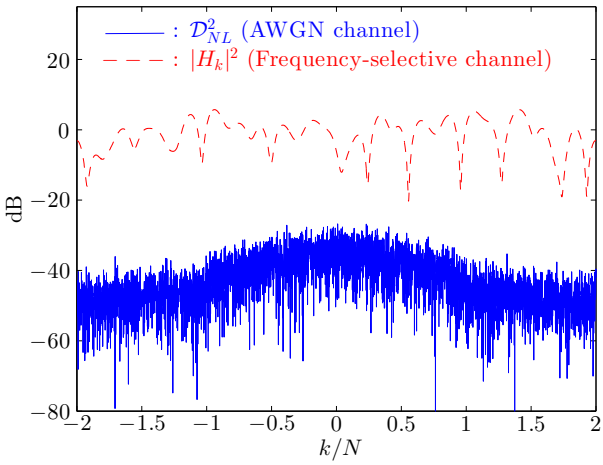

Fig. 7: Evolution of $\mathcal{D}_{NL}^2$ in an ideal AWGN channel and the channel frequency responses considering a frequency-selective channel with several multipath components.

Therefore, we have

$$\sum_k|H_k|^2\mathcal{D}_{d,k}^2 \approx \sum_k|H_k|^2\mathbb{E}[\mathcal{D}_{d,k}^2] \quad (46)$$
$$\approx \left(\frac{1}{NM}\sum_k|H_k|^2\right)\times\left(\sum_k\mathbb{E}[\mathcal{D}_{d,k}^2]\right),$$

where the first approximation comes from (a), (b) and (c) and the second approximation comes from (c), (d) and (e). Therefore,

$$\mathcal{G}_{H,c} \approx \frac{\frac{\mathbb{E}[\mathcal{D}_c^2]}{MN}\sum_{k=0}^{MN-1}|H_k|^2}{4E_b^{NL}} = \frac{\mathbb{E}[\mathcal{G}_c]\gamma_c}{NM}, \quad (47)$$

[7] This is not necessarily equal to $\sum_k\mathbb{E}[|H_k|^2]=NM$ due to statistical fluctuations in the amplitudes of the corresponding multipath components of that channel realization.

where

$$\gamma_c = \sum_{k=0}^{MN-1} |H_k|^2. \quad (48)$$

Our goal is to define the distribution of two random variables: γ_d, related to the frequency-responses that weight the discrete part of the gain, and γ_c, associated to continuous part of the gain. With these two distributions, we are in conditions to derive the distribution of the gain $\mathcal{G}_H$ and its basic statistical properties. Let us start by considering the general impulsive response of a frequency-selective channel with I multipath components given by

$$h(t) = \sum_{i=0}^{I-1} \alpha_i \delta(t - \tau_i), \quad (49)$$

where α_i and τ_i are the power and the delay of the i^{th} ray, respectively[8], and $\delta(\cdot)$ is the delta Dirac function. The corresponding channel frequency response is the Fourier Transform of $h(t)$, given by

$$H(f) = \sum_{i=0}^{I-1} \alpha_i \exp\left(-j2\pi f \tau_i\right), \quad (50)$$

and the channel frequency response associated to the k^{th} subcarrier is

$$H_k = H\left(f\right)|_{f=\frac{k}{T}} = \sum_{i=0}^{I-1} \alpha_i \exp\left(-j2\pi \frac{k}{T}\tau_i\right), \quad (51)$$

where T represents the duration of the OFDM symbol. As we consider that $\mathbb{E}\left[|H_k|^2\right] = \sum_{i=0}^{I-1} \mathbb{E}\left[|\alpha_i|^2\right] = 1$, the average power of the received signal is the same of the transmitted signal. Moreover, we assume uncorrelated Rayleigh fading on the different multipath components, i.e., $\alpha_i \sim \mathcal{CN}(0, \sigma_i^2)$ with $\sigma_i^2 = \frac{1}{I}$ for $i = 0, 1, ..., I-1$, and, consequently, $H_k \sim \mathcal{CN}(0, 1)$. The random variable $|H_k|^2$ is Gamma distributed with shape parameter $\omega = 1$ and scale parameter $\upsilon = 1$, i.e., $|H_k|^2 \sim \Gamma(1, 1)$ ($\mathbb{E}\left[|H_k|^2\right] = \omega\upsilon = 1$). Defined the distribution of $|H_k|^2$ we are in conditions to define the distribution of γ_d and γ_c. Regarding γ_c, we have $\gamma_c = \sum_{k=0}^{MN-1} |H_k|^2 \approx MN \sum_{i=0}^{I-1} |\alpha_i|^2$. This random variable has a Gamma distribution with shape parameter $\omega = I$ and scale parameter $\upsilon = \frac{MN}{I}$, i.e., $\gamma_c \sim \Gamma\left(I, \frac{MN}{I}\right)$. Similarly, from (45) we have $\gamma_d \sim \Gamma(\mu, 1)$. Fig. 8 shows the distribution of γ_c obtained both theoretically and by simulation, considering $I = 32$, $N = 512$ and $M = 4$. The figure confirms the high accuracy of our model for γ_c. In Fig. 9 it is shown the distribution $\mathcal{G}_{H,d}$ and $\mathcal{G}_{H,c}$ obtained both theoretically and by simulation, revealing that the theoretical expressions are accurate. The random variable $\mathcal{G}_H$ is given by the sum of two independent gamma variables with different parameters, i.e., $\mathcal{G}_{H,d} \sim \Gamma(\mu, \frac{\mathbb{E}[\mathcal{G}_d]}{\mu})$ and $\mathcal{G}_{H,c} \sim \Gamma(I, \frac{\mathbb{E}[\mathcal{G}_c]}{I})$. In Appendix. A we derive its distribution, that is

$$p(\mathcal{G}_H) = \frac{\left(\frac{\mu}{\mathbb{E}[\mathcal{G}_d]}\right)^{\mu}\left(\frac{I}{\mathbb{E}[\mathcal{G}_c]}\right)^{I}}{\Gamma(I+\mu)} \mathcal{G}_H^{I+\mu-1} \exp\left(-\frac{\mathcal{G}_H I}{\mathbb{E}[\mathcal{G}_c]}\right)$$

$$\times M\left(\mu, I+\mu, \mathcal{G}_H\left(\frac{I}{\mathbb{E}[\mathcal{G}_c]} - \frac{\mu}{\mathbb{E}[\mathcal{G}_d]}\right)\right), \quad (52)$$

[8]For the sake of simplicity, we assume that the multipath components are spaced by multiples of the sampling interval T/N.

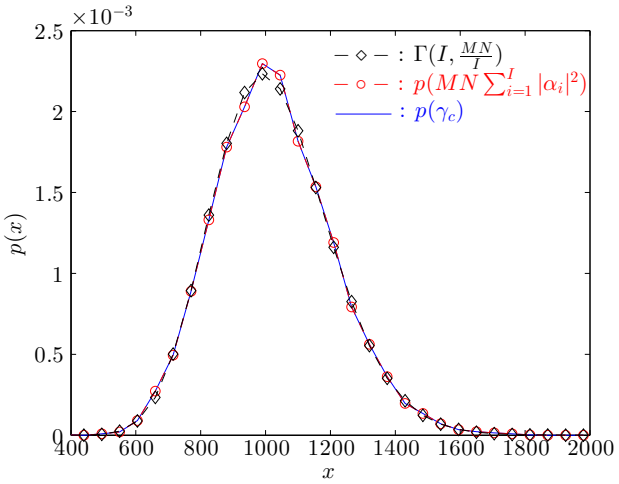

Fig. 8: Distribution of γ_c obtained both theoretically and by simulation.

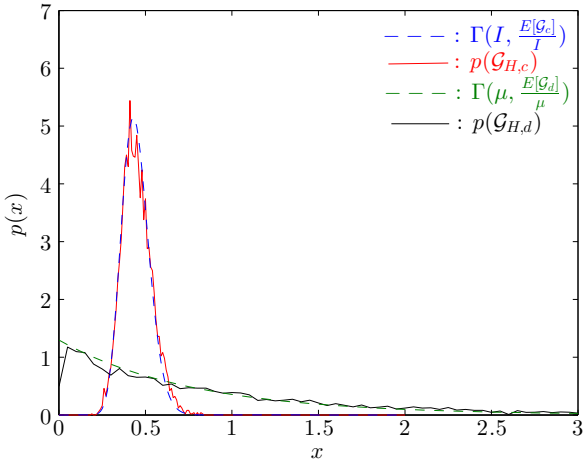

Fig. 9: Distribution of $\mathcal{G}_{H,d}$ and $\mathcal{G}_{H,c}$ obtained both theoretically and by simulation.

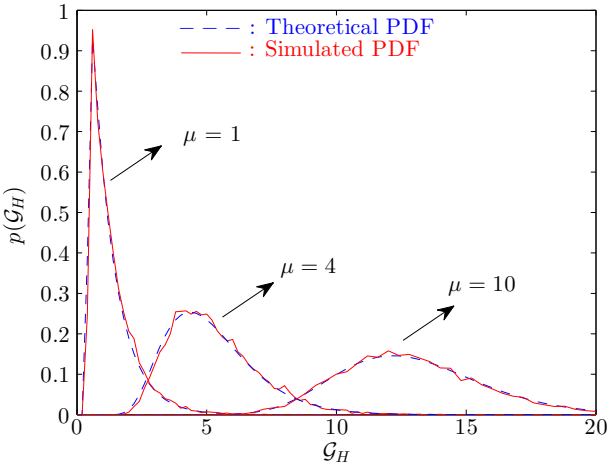

Fig. 10: Distribution of $\mathcal{G}_H$ obtained by simulation and with (52) considering different values of μ.

where $M(a,b,z)$ is the Kummer's function of the first kind [25]. In the next figures we present a set of results for the distribution of $\mathcal{G}_H$, $p(\mathcal{G}_H)$. Unless otherwise stated, it is assumed that the frequency-selective channel has $I = 32$ multipath rays with uncorrelated Rayleigh fading. The OFDM sequences have $N = 1024$ useful subcarriers, $M = 4$ and differ in μ bits. Fig. 10 it is shown the distribution of $\mathcal{G}_H$ obtained both theoretically and by simulation considering an envelope clipping parametrized with $s_M/\sigma = 1.0$. The figure shows the high accuracy of (52). As in the case of the ideal AWGN channel, higher values of μ lead to higher potential gains. It should be pointed out that as we are comparing with the AWGN channel results, when $\mu = 1$ we can have $\mathcal{G}_H < 1$, which also happens in the case of linear OFDM transmissions. Fig. 11 shows both the average value and the variance of $\mathcal{G}_H$ obtained theoretically and by simulation, which reinforces the accuracy of (52). Fig. 12 shows $p(\mathcal{G}_H)$ considering an ideal envelope clipping, $\mu = 1$ and different values of s_M/σ. Moreover, we also include $p(\mathcal{G}_H)$ considering a FDF after the nonlinearity (this distribution was obtained by simulation). From this figure, we note that even when there is a FDF that removes completely the out-of-band radiation, there are also high potential gains and we only have a slight degradation relatively to the unfiltered case. Additionally, it should be pointed out that the potential asymptotic gains obtained in frequency-selective channels are higher than the ones for ideal AWGN channels (see Fig. 4).

For $\mu = 5$ the average asymptotic gain is around 7.5 dB and for $\mu = 10$ (the free distance of a rate $1/2$ convolutional code) we have $\mathbb{E}[\mathcal{G}_H] \approx 11$ dB. The higher gains in frequency-selective channels can be explained due to the multipath diversity that increases when combined with the diversity inherent to the nonlinear distortion. Fig. 14 shows $p(\mathcal{G}_H)$ for a TWTA with $s_M/\sigma = 1.0$ and $\theta_M = \pi/3$. Since with this nonlinear characteristic we have stronger nonlinear distortion effects, the potential gains are also higher (see Fig. 6). Fig. 15 shows the asymptotic BER associated with the optimum detection in both AWGN and frequency-selective channels. This BER was obtained through the distributions of the gains $p(\mathcal{G})$ and $p(\mathcal{G}_H)$ when an ideal envelope clipping with $s_M/\sigma = 1.0$ is considered. For the sake of comparisons, we also include

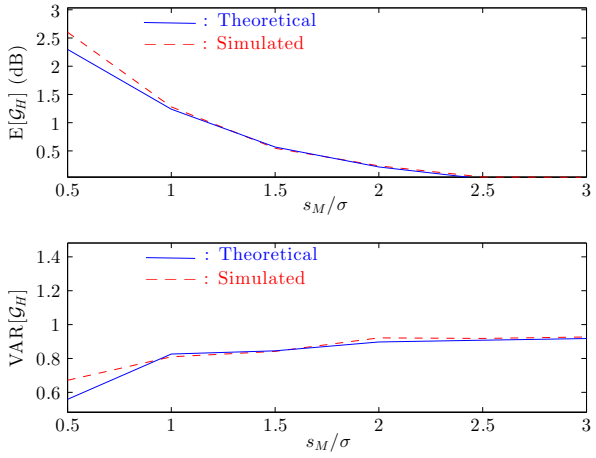

Fig. 11: $\mathbb{E}[\mathcal{G}_H]$ and $\mathrm{VAR}(\mathcal{G}_H)$ obtained theoretically and by simulation as a function of s_M/σ.

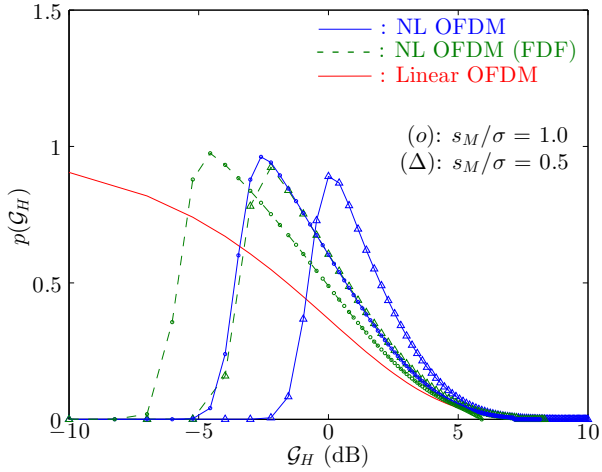

Fig. 12: Distribution of $\mathcal{G}_H$ considering different values of s_M/σ.

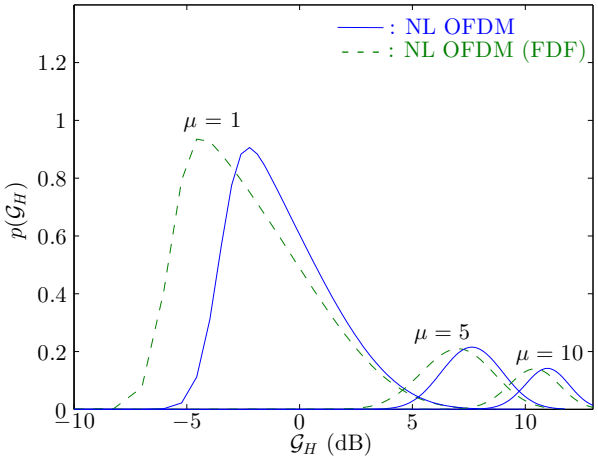

Fig. 13: Distribution of $\mathcal{G}_H$ considering an envelope clipping with $s_M/\sigma = 1.0$ and different values of μ.

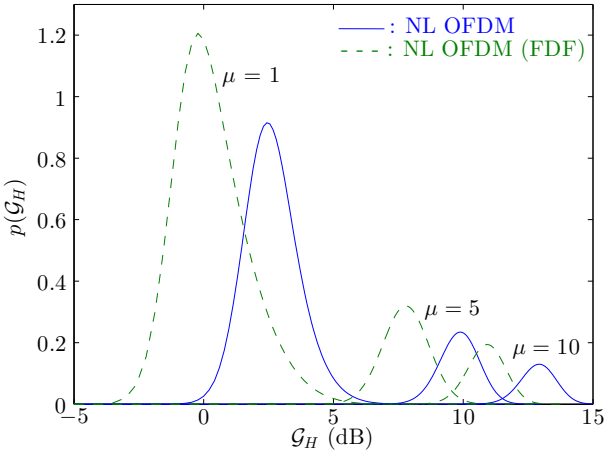

Fig. 14: Distribution of $\mathcal{G}_H$ considering a TWTA with $s_M/\sigma = 1.0$ and $\theta_M = \pi/3$.

the BER of the "Bussgang Receiver" [12], the sub-optimum receiver presented in [17], and a conventional receiver, as well as the performance of a linear OFDM transmission. The

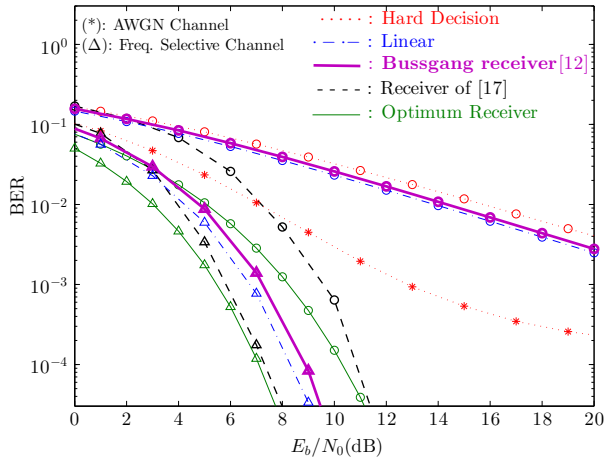

Fig. 15: BER considering a set of receivers and an envelope clipping with $s_M/\sigma = 1.0$ for both dispersive and non-dispersive channels.

very high potential gains associated to the gains distributions are traduced in significant BER improvements. Not only the optimum but also the sub-optimum receiver of [17] outperform all other receivers. For frequency-selective channels the gains are even higher due to the inherent diversity effect associated to the nonlinear distortion. The main weakness associated to the optimum receiver is its very high complexity. For instance, considering an $\mathcal{M}$ size constellation and N subcarriers, $\mathcal{M}^N$ data sequences must be analyzed before a decision. The reduced-complexity, sub-optimal receiver presented in [17] has a complexity of order $O(N\log_2(N))$ per data symbol, which might still be too high for most systems. For this reason, the design of efficient receivers that can explore the advantages of the nonlinear distortion and present low complexity is still an open aspect.

VI. Conclusions

In this paper we investigated the optimum performance of nonlinearly distorted OFDM signals when bandpass memoryless nonlinearities are employed at the transmitter. We presented analytical methods for obtaining the average asymptotic gain (when compared with OFDM signals with conventional, linear transmitters) and its distribution in frequency-selective channels with Rayleigh fading. Our analytical results were shown to be very accurate and indicate that the optimum detection of OFDM schemes with strong nonlinear distortion effects allows significant gains when compared with conventional, linear OFDM schemes. This means that we should not ignore the nonlinear distortion or treat it as an unavoidable annoyance, but as something that can help to improve the performance.

Appendix A
Demonstration of (52)

The random variable $\mathcal{G}_H$ is given by the sum of two independent gamma variables with different parameters, i.e., $\mathcal{G}_{H,d} \sim \Gamma(\mu, \frac{\mathbb{E}[\mathcal{G}_d]}{\mu})$ and $\mathcal{G}_{H,c} \sim \Gamma(I, \frac{\mathbb{E}[\mathcal{G}_c]}{I})$. [26] presents a general expression for the distribution of $Y = X_1 + X_2 + ... + X_n$, that represents the sum of n independent gamma variables in the form $X_i \sim \Gamma(\alpha_i = \omega_i, \beta_i = \frac{1}{\upsilon_i})$. In our case, we have $n = 2$ since we are summing two gamma variables. In these conditions, the general expression in [26] yields

$$p(y) = Cy^{\alpha_1+\alpha_2-1}\int_0^1 \exp(-yC_{\beta_1,\beta_2}(t))B_{\alpha_1,\alpha_2}(t)\mathrm{d}t, \quad (53)$$

with C given by

$$C = \frac{\beta_1^{\alpha_1}\beta_2^{\alpha_2}}{\Gamma(\alpha_1+\alpha_2)}, \quad (54)$$

$$C_{\beta_1,\beta_2}(t) = \beta_1 t + \beta_2(1-t), \quad (55)$$

$$B_{\alpha_1,\alpha_2}(t) = \frac{1}{B_2(\alpha_1,\alpha_2)}t^{\alpha_1-1}(1-t)^{\alpha_2-1}, \quad (56)$$

and

$$B_2(\alpha_1,\alpha_2) = \frac{\Gamma(\alpha_1)\Gamma(\alpha_2)}{\Gamma(\alpha_1+\alpha_2)}. \quad (57)$$

By using the last equations in (53), we may write

$$\begin{aligned} p(y) &= \frac{\beta_1^{\alpha_1}\beta_2^{\alpha_2}}{\Gamma(\alpha_1+\alpha_2)}y^{\alpha_1+\alpha_2-1}\int_0^1 \exp(-y(\beta_1 t+\beta_2(1-t))) \\ &\times \frac{1}{B_2(\alpha_1,\alpha_2)}t^{\alpha_1-1}(1-t)^{\alpha_2-1}\mathrm{d}t \\ &= \frac{\Gamma(\alpha_1+\alpha_2)}{\Gamma(\alpha_1)\Gamma(\alpha_2)}\frac{\beta_1^{\alpha_1}\beta_2^{\alpha_2}}{\Gamma(\alpha_1+\alpha_2)}y^{\alpha_1+\alpha_2-1}\exp(-y\beta_2) \\ &\times \int_0^1 \exp(yt(\beta_2-\beta_1))t^{\alpha_1-1}(1-t)^{\alpha_2-1}\mathrm{d}t. \end{aligned} \quad (58)$$

Introducing the variable $K = y(\beta_2 - \beta_1)$, we have

$$\begin{aligned} p(y) &= \frac{\beta_1^{\alpha_1}\beta_2^{\alpha_2}}{\Gamma(\alpha_1+\alpha_2)}y^{\alpha_1+\alpha_2-1}\exp(-y\beta_2)\frac{\Gamma(\alpha_1+\alpha_2)}{\Gamma(\alpha_1)\Gamma(\alpha_2)} \\ &\times \int_0^1 \exp(Kt)t^{\alpha_1-1}(1-t)^{\alpha_2-1}\mathrm{d}t. \end{aligned} \quad (59)$$

Using the definition of the Kummer's function of the first kind [25], $M(a,b,z)$, that is given by

$$M(a,b,z) = \frac{\Gamma(b)}{\Gamma(a)\Gamma(b-a)}\int_0^1 \exp(zu)u^{a-1}(1-u)^{b-a-1}\mathrm{d}u, \quad (60)$$

and knowing that $y = \mathcal{G}_H$, $a = \alpha_1$, $b = \alpha_1+\alpha_2$, $\alpha_1 = \mu$, $\alpha_2 = I$, $\beta_1 = \frac{\mu}{\mathbb{E}[\mathcal{G}_d]}$ and $\beta_2 = \frac{I}{\mathbb{E}[\mathcal{G}_c]}$, we can express $p(\mathcal{G}_H)$ as

$$\begin{aligned} p(\mathcal{G}_H) &= \frac{\left(\frac{\mu}{\mathbb{E}[\mathcal{G}_d]}\right)^{\mu}\left(\frac{I}{\mathbb{E}[\mathcal{G}_c]}\right)^{I}}{\Gamma(I+\mu)}\mathcal{G}_H^{I+\mu-1}\exp\left(-\frac{\mathcal{G}_H I}{\mathbb{E}[\mathcal{G}_c]}\right) \\ &\times M\left(\mu, I+\mu, \mathcal{G}_H\left(\frac{I}{\mathbb{E}[\mathcal{G}_c]}-\frac{\mu}{\mathbb{E}[\mathcal{G}_d]}\right)\right). \end{aligned} \quad (61)$$

REFERENCES

[1] L. Cimini Jr., "Analysis and simulation of a digital mobile channel using orthogonal frequency division multiplexing", *IEEE Trans. Commun.*, vol. 33, no. 7, pp. 665–675, July 1985.

[2] *Digital Video Broadcasting (DVB); framing structure, channel coding and modulation for digital terrestrial television*, ETSI Standard: EN 300 744 V1.6.1, Jan. 2009.

[3] *3rd Generation Partnership Project: technical specification group radio access network; physical layers aspects for evolved UTRA*, 3GPPP TR 25.814, Sept. 2006.

[4] *IEEE standard for local and metropolitan area networks - part 16: air interface for fixed broadband wireless access systems*, IEEE 802.16-2004, Oct. 2004.

[5] Y. Rahmatallah and S. Mohan, "Peak-to-average power ratio reduction in OFDM systems: a survey and taxonomy", *IEEE Commun. Surveys Tuts.*, vol. 15, no. 4, pp. 1567–1592, Mar. 2013.

[6] R. Dinis and A. Gusmão, "A class of nonlinear signal processing schemes for bandwidth-efficient OFDM transmission with low envelope fluctuation", *IEEE Trans. Commun.*, vol. 52, no. 11, pp. 2009–2018, Nov. 2004.

[7] A. Saleh, "Frequency-independent and frequency-dependent nonlinear models of TWT amplifiers", *IEEE Trans. Commun.*, vol. 29, no. 11, pp. 1715–1720, Nov. 1981.

[8] J. Armstrong, "New OFDM peak-to-average power reduction scheme", *IEEE VTC'2001 (Spring)*, Rhodes, Greece, May 2001.

[9] H. Ochiai and H. Imai, "Performance analysis of deliberately clipped OFDM signals", *IEEE Trans. Commun.*, vol. 50, no. 1, pp. 89–101, Jan. 2002.

[10] H. Rowe, "Memoryless nonlinearities with gaussian input: elementary results", *Bell System Tech. Journal*, vol. 61, no. 67, pp. 1519–1526, Sep. 1982.

[11] D. Dardari, V. Tralli and A. Vaccari, "A theoretical characterization of nonlinear distortion effects in OFDM systems", *IEEE Trans. Commun.*, vol. 48, no. 10, pp. 1755–1764, Oct. 2000.

[12] A. Gusmão and R. Dinis, "Iterative receiver techniques for cancellation of deliberate nonlinear distortion in OFDM-type transmission", *IEEE Int. OFDM Workshop'04*, Dresden, Germany, Sep. 2004.

[13] A. Gusmão, R. Dinis and P. Torres, "Low-PMEPR OFDM transmission with an iterative receiver technique for cancellation of nonlinear distortion", *IEEE VTC'2005 (Fall)*, Dallas, USA, Sep. 2005.

[14] J. Tellado, L. Hoo and J. Cioffi, "Maximum likelihood detection of nonlinearly distorted multicarrier symbols by iterative decoding", *IEEE Trans. Commun.*, vol. 51, no. 2, pp. 218–228, Feb. 2003.

[15] Z. Kollár, M. Grossmann and R. Thomä, "Convergence analysis of BNC turbo detection for clipped OFDM signaling", in *Proc. of the 13th International OFDM-Workshop (InOWo'2008)*, Hamburg, Germany, Aug. 2008.

[16] F. Peng and E. Ryan, "MLSD bounds and receiver designs for clipped OFDM channels", *IEEE Trans. Wireless Commun.*, vol. 7, no. 9, pp. 3568–3578, Sep. 2008.

[17] J. Guerreiro, R. Dinis and P. Montezuma, "Optimum and sub-optimum receivers for OFDM signals with strong nonlinear distortion effects", *IEEE Trans. Commun.*, vol. 61, no. 9, pp. 3830–3840, Sep. 2013.

[18] J. Guerreiro, R. Dinis and P. Montezuma, "Approaching the maximum likelihood performance with nonlinearly distorted OFDM signals", *IEEE VTC'2012 (Spring)*, Yokohama, Japan, May 2012.

[19] J. Guerreiro, R. Dinis and P. Montezuma, "Optimum and sub-optimum receivers for OFDM signals with iterative clipping and filtering", *IEEE VTC'2012 (Fall)*, Québec City, Canada, Sep. 2012.

[20] G. Santella and F. Mazzenga, "A model for performance evaluation in M-QAM-OFDM schemes in presence of nonlinear distortions", *IEEE VTC'1995*, Chicago, USA, July 1995.

[21] E. Costa, M. Midrio and S. Pupolin, "Impact of amplifier nonlinearities on OFDM transmission system performance", *IEEE Comm. Let.*, vol. 3, no. 2, pp. 37–39, Feb. 1999

[22] P. Banelli and S. Cacopardi, "Theoretical analysis and performance of OFDM signals in nonlinear AWGN channels", *IEEE Trans. Commun.*, vol. 48, no. 3, pp. 430–441, Mar. 2000.

[23] S. Chen and T. Yao, "FEQ for OFDM systems with insufficient CP", *Proc. IEEE Pers., Indoor, Mobile Radio Commun. 2003*, Beijing, China, Aug. 2003.

[24] S. Chen and C. Zhu, "ICI and ISI analysis and mitigation for OFDM systems with insufficient cyclic prefix in time-varying channels", *IEEE Trans. Consumer Electronics*, vol. 50, no. 1, pp. 78–83, Feb. 2004.

[25] M. Abramowitz and I. A. Stegun, *Handbook of Mathematical Functions*. New York: Dover, 1965.

[26] M. Akkouchi, "On the convolution of gamma distributions", *Soochow Jornal of Matematics*, vol. 31, no. 2, pp. 205–201, Apr. 2005.

João Guerreiro received the MSc. degree from Faculdade de Ciências e Tecnologia (FCT), Universidade Nova de Lisboa (UNL), in 2012. He is currently a Ph.D. student at Faculdade de Ciências e Tecnologia (FCT), Universidade Nova de Lisboa (UNL). His research interests include multicarrier communications and nonlinear distortion effects.

Rui Dinis (M'00, SM'14) received the Ph.D. degree from Instituto Superior Técnico (IST), Technical University of Lisbon, Portugal, in 2001 and the Habilitation in Telecommunications from Faculdade de Ciências e Tecnologia (FCT), Universidade Nova de Lisboa (UNL), in 2010. From 2001 to 2008 he was a Professor at IST. Currently he is an associated professor at FCT-UNL. During 2003 he was an invited professor at Carleton University, Ottawa, Canada. He was a researcher at CAPS (Centro de Análise e Processamento de Sinal), IST, from 1992 to 2005 and a researcher at ISR (Instituto de Sistemas e Robótica) from 2005 to 2008. Since 2009 he is a researcher at IT (Instituto de Telecomunicações). Rui Dinis is editor at IEEE Transactions on Communications (Transmission Systems - Frequency-Domain Processing and Equalization) and guest editor for Elsevier Physical Communication (Special Issue on Broadband Single-Carrier Transmission Techniques). He has been actively involved in several international and national research projects in the broadband wireless communications area. His research interests include modulation, equalization, channel estimation and synchronization.

Paulo Montezuma Paulo Montezuma received the Ph.D. degree from FCT-UNL (Faculdade de Ciências e Tecnologia da Universidade Nova de Lisboa), in 2007. Since 2001 he is teaching at the Department of Electrical Engineering (DEE) of the FCT. From 1996 to 2005 he was a researcher at CAPS/IST (Centro de Análise e Processamento de Sinais/Instituto Superior Técnico). In 2001 he joined the Uninova-CTS research centre. He has been involved in several research projects in Telecommunications area, both national and European. His main research interests include modulation, channel coding, signal design for wireless communications, nonlinear effects and spread spectrum systems.